



Published in final edited form as:

Nat Neurosci. 2013 December ; 16(12): 1888–1895. doi:10.1038/nn.3549.

Common medial frontal mechanisms of adaptive control in humans and rodents

Nandakumar S. Narayanan^{#1}, James F. Cavanagh^{#2}, Michael J. Frank^{2,3}, and Mark Laubach^{4,*}

¹Department of Neurology, Carver College of Medicine, The University of Iowa

²Cognitive, Linguistic & Psychological Sciences, Brown Institute for Brain Science, Psychiatry and Human Behavior, Brown University

³Department of Psychiatry, and Brown Institute for Brain Science, Brown University

⁴The John B. Pierce Laboratory and Department of Neurobiology, Yale University School of Medicine

These authors contributed equally to this work.

Abstract

In this report, we describe how common brain networks within the medial frontal cortex facilitate adaptive behavioral control in rodents and humans. We demonstrate that low frequency oscillations below 12 Hz are dramatically modulated after errors in humans over mid-frontal cortex and in rats within prelimbic and anterior cingulate regions of medial frontal cortex. These oscillations were phase-locked between medial frontal cortex and motor areas in both rats and humans. In rats, single neurons that encoded prior behavioral outcomes were phase-coherent with low-frequency field oscillations particularly after errors. Inactivating medial frontal regions in rats led to impaired behavioral adjustments after errors, eliminated the differential expression of low frequency oscillations after errors, and increased low-frequency spike-field coupling within motor cortex. Our results describe a novel mechanism for behavioral adaptation via low-frequency oscillations and elucidate how medial frontal networks synchronize brain activity to guide performance.

INTRODUCTION

Adaptive control allows an agent to change behavior in order to improve performance after mistakes are made^{1,2}. This process involves guiding behavior according to a previous outcome, and is commonly associated with prediction error signaling in medial frontal areas

Users may view, print, copy, download and text and data- mine the content in such documents, for the purposes of academic research, subject always to the full Conditions of use: http://www.nature.com/authors/editorial_policies/license.html#terms

*Correspondence and requests for materials should be addressed to: Mark Laubach, Ph.D., The John B. Pierce Laboratory, 290 Congress Avenue, New Haven, CT 06519, 203-401-6202 (voice), 203-624-4950 (fax), mlaubach@jbpierce.org.

Contributions: NN, JC, MF and ML designed experiments and wrote the paper. NN and JC conducted experiments. NN, JC and ML analyzed data.

Disclosure: The authors report no competing financial interests.

such as the anterior cingulate cortex (ACC)^{3,4}. Adaptive control is compromised in a number of psychiatric and neurological disorders, such as schizophrenia, Attention Deficit-Hyperactivity Disorder (ADHD), Obsessive Compulsive Disorder (OCD), Parkinson's disease, and schizophrenia^{2,5-7}. However, our understanding of these deficits is hindered by a lack of knowledge of the specific mechanisms by which the medial frontal cortex adjusts performance based on prior outcome. Here we describe how common features of adaptive control in rodents and humans appear to be mediated by medial frontal low-frequency oscillations. This similarity allowed us to utilize cross-species comparisons to explore candidate mechanistic processes by which medial frontal regions guide behavior.

Medial frontal cortex has been demonstrated to guide behavior according to behavioral goals⁸⁻¹⁰ and monitor behavioral states^{2,11} in the service of optimal performance^{12,13}. For instance, in reaction time tasks, participants typically engage in a deliberative speed-accuracy tradeoff if the previous trial was an error, a phenomenon known as post-error slowing¹⁴⁻¹⁶. Interestingly, rodents also exhibit post-error slowing after errors¹¹. In both rodents and humans, lesions in medial frontal cortex impair such processes^{11,13,17}. Clearly, a detailed understanding of the specific mechanism by which the medial frontal cortex improves performance would facilitate understanding, diagnosis, and treatment for diseases associated with impaired adaptive control^{18,19}.

In the present study, we recorded from medial frontal and motor networks in both rodents and humans during a simple time-estimation task. This novel cross-species approach allowed us to characterize a conserved neuro-behavioral repertoire across mammalian species, and provided mechanistic insight into how medial frontal networks guide behavior in accordance with behavioral goals. We found that rats and humans exhibited similar enhancement of low-frequency oscillations after errors in a time-estimation task and that these neural signals commonly related to trial-by-trial behavioral adaptation. Most importantly, pharmacological disruption of rodent medial frontal cortex eliminated the selective expression of post-error low-frequency oscillations in the motor cortex, as well as adaptive post-error behavioral adjustment.

RESULTS

Similar post-error signals in humans and rodents

To examine the relationship between error-related activity in humans and rodents, we recorded neural activity using a time-estimation task (Fig 1a), in which a response was required at an estimated time interval (human: 1.4 sec, rat: 1 sec) and an imperative stimulus (tone) was presented at the target time on 50% of trials²⁰. Humans and rodents had comparable response latencies from the target time (236 ± 18 ms for humans vs 250 ± 40 ms for rats, mean \pm standard error) but somewhat different premature error rates ($7 \pm 1\%$ for humans vs $25 \pm 3\%$ for rats).

In 11 humans, we recorded 64-channel scalp EEG while they performed this task. We then compared event-related potentials (ERPs) on trials after correct and premature error responses (post-correct and post-error trials, respectively; Fig 1a). Human ERPs were measured by the difference between the mean of the first major peak (P3: 275 ms \pm 25

ms) and the preceding trough (N1: 125 ms \pm 25 ms), which corresponds to an approximate frequency of 6Hz. On post-error trials, humans had significantly larger mid-frontal ERPs to the target time as compared to trials preceded by correct responses (paired t-test $t_{(10)}=2.75$: $p<.02$; Fig 1b).

We compared these signals to intracortical field potentials recorded from 28 channels in the medial frontal cortex of 5 rodents (Fig S1). Strikingly, intracortical local field potentials in rodents had a nearly identical pattern to humans during the response period (Fig 1c), with enhanced ERPs on post-error trials compared to post-correct trials (paired t-test $t_{(27)}=1.90$, $p < 0.04$). These data suggest a common neural mechanism of adaptive control in rodents and humans.

Spectral analysis of post-error signals

To investigate the spectral dynamics of post-error adjustments, we examined the time-frequency power spectra of human electroencephalograms (EEG) and rodent local field potentials (LFPs) on post-correct and post-error trials (Fig 2a-b). This analysis directly compared power spectra over time on post-error trials with power spectra on post-correct trials. In humans, theta power (4-8 Hz) over mid-frontal leads was present on all trials (Fig 2a), but it was much stronger on post-error trials (Fig 2c; outlined areas: $p<0.05$). If theta power indicates a signal related to behavioral adjustment, then it may be expected to correlate with response time adjustments. Indeed, we found mid-frontal theta-band power was more strongly correlated with response time adjustments on post-error compared to post-correct trials (Fig 2d). Topographic plots of current density revealed that these relationships occurred over mid-frontal sites, corresponding to generative sources from medial frontal cortex and recapitulating findings from previous humans studies²¹.

In rodents, time-frequency analysis also revealed strong low-frequency power on all trials (below 12 Hz; Fig 2b). These frequencies were specifically enhanced on post-error compared to post-correct trials (Fig 2e). As in humans, trial-to-trial power in theta to beta ranges (Fig 2f; 4-25 Hz) was more strongly correlated with response time adjustments on post-error compared to post-correct trials. Taken together, these data suggest that humans and rodents share features of adaptive control via low-frequency oscillations in the medial frontal cortex.

Interactions between medial frontal cortex and motor cortex

Adaptive control signals from the medial frontal cortex must access the motor system to exert control over action. Synchronous field oscillations have been shown to entrain activity across distant brain regions^{22,23}, providing a candidate mechanism for top-down prefrontal control over motor cortex^{8,10,21}. Neurons in the rodent motor cortex have been shown to encode variations in reaction time performance^{24,25} and are influenced by top-down input from the medial frontal cortex¹⁰. We used spectral coherence methods to examine interactions between the medial frontal and motor cortices in the time-estimation task. In humans, inter-site phase coherence was significantly increased between mid-frontal leads and motor sites contralateral to the response hand on post-error compared to post-correct trials (Fig 2g). This difference between conditions was absent, and even slightly reversed,

when tested at an intermediary site (Fig S2), demonstrating that this effect was not due to volume conduction. In the rodent study, we simultaneously recorded 12 medial frontal fields and 12 motor cortex fields in 3 animals. As in the human study, inter-site phase coherence was significantly increased on post-error compared to post-correct trials (Fig 2h). Together, our findings in the human and rat studies are consistent with previous findings which suggest that low frequency oscillations act as a mechanism for entraining activity between medial frontal and motor cortex in service of adaptive control of performance²⁶.

Medial frontal neurons and fields are coherent only after errors

Next, we investigated if the spike activity of neurons in the medial frontal cortex was linked to the observed increase in low-frequency power after errors. Local field oscillations facilitate rhythmic excitability of neurons and can create temporal windows for organizing functional ensembles of neurons^{23,27}. Spike-triggered averages of medial frontal field potentials revealed that spikes on post-error trials have robust low-frequency coupling when compared to spikes on post-correct trials (Fig 3a). For many neurons, firing rates were elevated on post-error trials and trial-averaged spike density functions exhibited temporal fluctuations (Fig 3b). To examine the dynamics of this functional coupling, we used spike-field coherence²⁸ to analyze relationships between 81 medial frontal neurons and 28 medial frontal field potentials simultaneously recorded from 5 animals. This analysis investigates trial-by-trial relationships of time-frequency coherence between single neuronal activity and the local field potential (Fig 3c&d). We found that spike-field coherence was much stronger on post-error compared to post-correct trials (Fig 3d-e: no spike-field pairs with significant coherence on post-correct trials vs. 7 pairs on post-error trials; $X^2 = 7.31$, $p < 0.007$), particularly between 2 and 13 Hz (Fig 3d). These findings demonstrate that single medial frontal neurons can be entrained to low-frequency local field oscillations that are elevated on post-error trials.

Neurons in the medial frontal cortex encode adaptive control

To further explore the cellular basis of adaptive control, we investigated the spiking activity of single units from rodent frontal cortex as a function of previous outcome using partial correlation analysis. We analyzed activity from 94 units from the medial frontal cortex in 6 animals and 87 units from the motor cortex in 5 rats. Partial correlation analysis was used to measure the relationship between the firing rate of each neuron and two behavioral variables (prior outcome and current response latency). Prior outcome was measured as the duration of the response on the previous trials, which was less than 1 sec for premature responses. Partial correlation analysis was carried out using the Matlab function `partialcorr` and correlation was measured using Spearman's rank-correlation. By using partial correlation, we were able to isolate effects of the prior outcome that were independent of the current response time, and vice versa. To isolate the effects of each behavioral variable, the analysis fit a least squares regression model to explain the effects of one behavioral variable (e.g. the response times) on spike counts measured in a sliding data window around the task events. Then a second regression model was fit to explain the effects of the other behavioral variable (e.g. previous outcome) on the residual variance (e.g. due to response times). We used a 200 ms data window to measure firing rates and a step size of 50 ms.

The partial correlation analysis revealed clear examples of neurons that varied with the previous behavioral outcome in both the medial frontal and motor cortices (Fig 4a). In both cortical areas, there was a steady encoding of the previous behavioral outcome throughout the period before the trial (Fig 4b). Neurons in the motor cortex, but not the medial frontal cortex, later encoded the response latency on the current trial (Fig 4b). Overall the entire trial epoch (± 2 sec around the lever press), slightly more neurons in the medial frontal cortex were sensitive to the previous behavioral outcome ($X^2=2.86$, $p<0.1$) and significantly more neurons in the motor cortex were sensitive to response latency ($X^2=17.75$, $p<0.001$; left bars in Fig 4c). However, as there was a clear sequential effect of the previous behavioral outcome in this task, we examined the fractions of cells that were exclusively sensitive to previous outcomes and response latency on the current trial. There was a clear difference in the encoding of these behavioral measures between the medial frontal and motor cortices (right bars in Fig 4c). More neurons in the medial frontal cortex exclusively encoded the previous behavioral outcome ($X^2=21.47$, $p<0.001$). By contrast, more neurons in the motor cortex exclusively encoded response latency ($X^2=8.22$, $p<0.01$).

These effects of prior outcomes were also apparent in local field potential recordings from the medial frontal cortex. For example, event-related potentials synchronized to the start of the trial were larger on post-error trials compared to post-correct trials, and showed clearly that low frequency rhythms in the pre-trial period (Fig 4d: whereas the LFPs in Fig 1c were time-locked to the target time, here they were time-locked to lever press). Spectral analysis revealed elevated low-frequency power (below 8 Hz) around the response on post-error trials (paired t-test $t_{(5)}=-4.23$, $p<0.001$; Fig 4e; Fig S3). Together, these findings suggest that neuronal activity in the medial frontal cortex encodes information that is involved in monitoring performance and that could influence the control of response adjustments by the motor cortex.

Inactivation of medial frontal cortex eliminates adaptive control

To test the causal and directional nature of medial frontal control over motor cortex, we recorded from motor cortex while inactivating medial frontal cortex using muscimol²⁹, an approach that we have described in extensive detail previously^{10,11,29,30}. In six rats, inactivating the medial frontal cortex resulted in more premature errors (paired t-test $t_{(5)}=-6.14$, $p<0.002$) and reduced overall response latencies (paired t-test $t_{(5)}=4.01$, $p<0.02$; Fig 5a). Overall behavioral performance was much more erratic in inactivation sessions, which resulted in more consecutive premature errors and therefore complicated the analysis of sequential effects. Rats showed overall speeding of response latencies in medial frontal inactivation sessions after making correct responses (median adjustment for the 6 rats in Control sessions: -0.01 sec, inactivation sessions: -0.180 sec; paired t-test: $t=2.77$, $p<0.04$). To ensure that the behavioral effects of medial frontal inactivation were not due to the erratic performance in the inactivation sessions, we searched for sequences of trials in which the rats performed three consecutive correct responses or made a premature error and then made two consecutive correct responses (Fig 5b). In control sessions, there was clear evidence for post-error slowing (paired t-test $t_{(5)}=-2.58$; $p<0.05$) and a subsequent post-correct speeding of performance after the next correct response (paired t-test: $t=3.86$, $df=5$, $p<0.01$; left plot in Fig 5c). Strikingly, in medial frontal inactivation sessions rats showed an

overall speeding of response latencies and this eliminated both the post-error slowing and subsequent post-correct speeding (right plot in Fig 5c; paired t-tests all with $p > 0.1$). Post-error response latencies were faster in inactivation sessions (paired t-test $t_{(5)} = 2.75$, $p < 0.04$; Fig 5c) while post-correct response latencies were unchanged sessions (paired t-test $t_{(5)} = 0.88$, $p < 0.42$).

In summary, these behavioral analyses establish that the medial frontal cortex is crucial for the adaptive control of RTs. In the absence of medial frontal function, rats show (1) an overall speeding of RTs, (2) an enhanced speeding of performance after correct responses, and (3) a loss of post-error adjustments. In the sections below, we investigate neural activity in the motor cortex in the absence of medial frontal control.

Inactivation of medial frontal cortex eliminated error-selective activity in the motor cortex

In three rats, we simultaneously inactivated medial frontal cortex while recording field potentials and single units in the motor cortex. Analysis of field potentials from 19 channels across 3 animals revealed a differential expression of low frequency oscillations on post-error trials (Fig 6a). Peri-event averages of bandpass filtered (2-8 Hz) LFPs showed a clear enhancement of oscillatory content on post-error trials (bottom row in Fig 6a); with a larger power envelope of the oscillations as derived by Hilbert transform (Control sessions, paired t-test $t_{(18)} = -3.62$, $p < 0.002$; inactivation sessions, paired t-test $t_{(18)} = -0.19$, $p > 0.8$; Ratio of inactivation to control, paired t-test $t_{(18)} = 5.3$, $p < < 0.001$; Fig 6b). Surprisingly, these differential signals were eliminated when the medial frontal cortex was inactivated (Fig 6a-b). Spectral analysis of the motor cortex LFPs showed that medial frontal inactivation eliminated the power enhancement on post-error trials (Fig 6c; Fig S4). Together, these results suggest that low frequency oscillations in the motor cortex were uncoupled from prior outcomes when the medial frontal cortex was inactivated.

Motor cortex spike-field coherence requires medial frontal cortex

To examine how spike activity in the motor cortex was affected by medial frontal inactivation, we used spike-field coherence to examine spike activity from 58 neurons in the control sessions and 61 neurons in medial frontal inactivation sessions. Under control conditions, there was increased post-error spike-field coherence compared to post-correct trials (Fig 7a-c; 10 spike-field pairs with significant coherence on post-error trials vs. 1 on post-correct trials; $X^2 = 8.1$, $p < 0.004$). Similar to the LFP results (Fig S4; Fig 6a), strong spike-field coherence was seen both on post-correct trials (Fig 7c; 45 spike-field pairs had significant coherence) and post-error trials (31 pairs post-error; $X^2 = 6.8$, $p < 0.009$; different from control sessions; $X^2 = 20.5$, $p < < 0.001$; Fig S5).

While there were clear consequences of inactivating the medial frontal cortex on spike-field coherence in the motor cortex, there was no effect on the basic firing properties of motor cortex neurons¹⁰. To investigate the predictive relationship of motor cortex with response time and medial frontal inactivation, we used partial correlation as in Fig 4. We found no effects of inactivation on the average correlation between firing rates and prior outcomes or current response latencies (Fig 7d; note that these data are a subset of Fig 4b) and no difference in the fractions of cells that exhibited significant correlations between firing rate

and the two behavioral measures (firing rate: $X^2 = 0.56$, $p=0.46$; prior outcomes: $X^2 = 0.35$, $p=0.55$ $X^2 = 0.10$, $p=0.75$;). Therefore, our results suggest that the medial frontal cortex achieves adaptive control over action by altering the coupling between spike activity and low frequency oscillations, but not the firing rates of neurons, in the motor cortex.

In summary, these findings demonstrate that with medial frontal cortex inactivated, motor cortex spike-field coherence is no longer specific to post-error trials and is decoupled from variance in response latency (see Fig S6 for a summary). This suggests that adaptive control of low-frequency coherence in motor cortex requires medial frontal activity. These findings provide unique causal evidence for the idea that the medial frontal cortex exerts adaptive control over motor cortex, and implicates low-frequency oscillatory coupling as a mechanism for realization and communication of the need for adaptive control across distant brain regions.

DISCUSSION

The findings reported here provide novel evidence that that low-frequency oscillations within medial frontal cortex: (1) are increased after errors (Fig 2b and Fig 2e), (2) predict adaptive control over response time (Fig 2c and 2f), (3) synchronize local neurons that contain information about the need for adaptive control (Figs 3-4), (4) are coherent with oscillations in motor cortex that contain information about behavioral adaptation (Figs 2g-h and Fig 4), and (5) have a causal role in this process (Figs 5-7). To the extent possible using non-invasive recordings, we demonstrated these same findings (#1, 2, & 4 above) in humans performing a highly similar task. While prior work has shown medial frontal correlations between prior outcome and response time^{13,17} in humans and rodents as well as coupling between local field potentials and single neurons²³, this is the first study to integrate these findings and demonstrate common mechanisms of behavioral adaptation in rodents and humans.

Causal evidence for the role of medial frontal oscillations in adaptive control was found by reversibly inactivating the rat medial frontal cortex using muscimol. Inactivating the medial frontal cortex resulted in (1) a speeding of response times especially after correct responses, (2) a loss of behavioral adjustments after errors (Fig 5c), (3) an overall increase in low frequency oscillations and the loss of selective elevations in low frequency power after errors (Fig 6), (4) a loss of the selective increase in phase locking between spikes and fields in the motor cortex on post-error trials (Fig 7a&b), and (5) an overall increase in phase locking between spikes and fields (Fig 7c). Interestingly, these effects occurred in the absence of changes in firing rate correlates of prior outcomes or response times in the motor cortex (Fig 7d). These findings suggest that low-frequency oscillations facilitate synchronization among brain networks for representing and exerting adaptive control³¹⁻³³, including top-down regulation of behavior⁷, in the mammalian brain.

Previous studies^{11-13,21,32}, in rats and humans, have reported evidence for post-error changes in processing in the medial frontal cortex. However, to our knowledge, this is the first direct comparison of rodent and human neural signals during the performance of a similar behavioral task and the first demonstration of common mechanisms for adaptive

control in these two species. We report remarkably comparable ERPs and common low-frequency elements from microelectrodes in rodent frontal cortex and human EEG, suggesting that adaptive control is a conserved behavioral repertoire arising from medial frontal cortex³⁴.

While rodents appeared to have broad-band low-frequency power alterations related to adaptive control, humans had rather selective alterations within the theta band. It is notable that these species shared common features in the ERP, in correlation between low-frequency power and reaction time, and in coherence between prefrontal and motor regions. However, these comparisons are ultimately based on different signals, as the rat LFP arises from intracortical local-field potentials placed directly within layer II/III and the EEG leads are placed on the scalp some distance away from generative sources. Although scalp electrodes (in humans) and local microelectrodes (in rodents) are certainly sampling contributions from distinct anatomical areas, the concordance between these two signals is compelling and suggests a shared network for error-related adjustment.

It is encouraging to observe that errors are a common trigger of low-frequency oscillations, which are reliably correlated with performance-adjustments. These results imply a common-basis for behavioral adjustment after errors. However, brain networks vastly differ between humans and rodents. Furthermore, these species might use distinct behavioral strategies to perform this task. Future investigation of field potentials from depth electrodes from human intraoperative recordings and recordings in other animal models such as mice will shed light on the generality of these findings. Regardless, this conservation of functional neural resources facilitates an increasingly mechanistic understanding of human error-processing using animal models. The development of such an animal model of adaptive control may provide tremendous benefit for the investigation of diseases characterized by impaired adaptive control such as OCD⁷, depression³⁵, ADHD⁹, Parkinson's disease³³, and schizophrenia¹⁹, and for investigating dimensional aspects of these diseases such as impulsivity and effortful control

These findings lend novel support to the idea that low-frequency oscillations represent the mechanism by which adaptive control is instantiated in prefrontal networks^{21,27}. Low frequency oscillations, particularly in the theta band, have been commonly seen after humans make errors in a variety of contexts²¹. We found that low-frequency oscillations synchronize medial frontal neurons, and medial frontal neurons are correlated with and control low-frequency oscillations in motor cortex at a trial-by-trial level. Interestingly, when medial frontal cortex was inactivated, low-frequency spike-field coherence in motor cortex was more robust and was no longer specific to post-error trials. Thus, with medial frontal cortex inactivated, animals may be functioning in a mode that is less flexible, and they may not benefit from information about previous outcome. These findings not only suggest that prefrontal regions regulate low-frequency coherence related to adaptive control in downstream areas such as motor cortex, but they indicate that low-frequency coupling is required for behavioral adjustments after animals make errors. Our results support the idea that low frequency oscillations are a candidate mechanism by which large populations of neurons can be synchronized across diverse brain regions in order to adjust behavior.

The medial frontal and motor areas reported here are not robustly connected³⁶. In rats, there are connections between the medial frontal cortex and rostral part of the motor cortex (i.e. the rostral forelimb area) which could mediate adaptive control over action. The medial frontal and motor cortices may also share a thalamic relay to facilitate transient increases in phase consistency³⁷. Such phase-dependent coupling may synchronize multiple cortical and subcortical structures²³, and may originate from either synaptic activity within cortical layers, or from subcortical inputs, such as thalamic³⁷, monoaminergic³⁸, or cholinergic³⁹ projections. The circuit through which the medial frontal cortex accesses the motor cortex is at present unknown; however, the findings reported in the present study establish that the low-frequency network dynamics of the motor cortex are regulated by activity in the medial frontal cortex. Specifically, medial frontal inactivation eliminated post-error adjustments and abolished the specificity of low-frequency spike-field coupling on post-error trials.

The finding of generalized and enhanced motor spike-field coherence with medial frontal inactivation suggests the involvement of additional circuits that contribute to adaptive control. Future studies will record from cortical areas in combination with key structures such as the thalamus and the subthalamic nucleus³³ to identify the full source and relay of adaptive control signals. Given that these low-frequency oscillations appear to be important for optimal behavioral performance, these efforts may illuminate pharmacological therapeutic opportunities that may benefit patients with impaired adaptive control.

In summary, we have detailed how low-frequency oscillations in rodent medial frontal cortex are modulated after errors and are coherent with single neurons across neural areas, providing a candidate mechanism for entraining functional networks in the service of behavioral control. Many of the core features of this system appear to be preserved in humans. This conserved neuro-behavioral repertoire across mammalian species provides an appealing translational model for testing novel pharmacological and stimulation techniques⁴⁰ that may contribute to treatment of diseases with impaired adaptive control.

METHODS

Human EEG

A total of 12 adults were recruited from the Brown University undergraduate subject pool and Providence community to complete the experiment (6 male; age $M=21$, $SD=2.22$). All participants had normal or corrected-to-normal vision, no history of head trauma or seizures, and were free from current psychoactive medication use. Data from one participant was excluded for having too few errors, yielding a final N of 11 participants. No statistical methods were used to pre-determine sample sizes but our sample sizes are similar to those reported in previous publications^{21,32,33,41}. Informed consent was obtained and all procedures complied with the Institutional Review Board at Brown University.

Human time-estimation task

Participants were informed that they were expected to estimate a time period of 1.4 seconds. An irregular time interval was chosen to ameliorate the influence of simple counting for time estimation. Participants were also informed that on half of the trials, an imperative tone

(MATLAB *beep* command) would be played at the target time and they were to respond as soon as possible in that instance. All trials began with a white fixation cross. After a varied ITI (100 to 1500 ms), the cross turned blue indicating that participants could initiate the next trial. Participants began each trial by pressing the left joystick button; they then used the right button to signal their response. If they responded too early (errors) or too late (too-slow), they received feedback indicating they were ‘Incorrect’ (for 1000 ms, varied from 200-400 ms after the response) and had an additional post error timeout of 2000 ms. Unbeknownst to the participants, the response latency window varied using an adaptive algorithm that aimed to keep a 20% error rate (error and too-slow). Participants completed 500 trials total. Late and post-late responses were not analyzed.

EEG Recording and Preprocessing

EEG was recorded using a 64 channel Brain Vision system. EEG was recorded continuously with hardware filters set from 0.1 to 100 Hz, a sampling rate of 500 Hz, and an online reference posterior to the vertex. Data windows for the continuous EEG recordings were placed around the onset of each trial (–1500 ms to 6000 ms). Data were then visually inspected to identify bad channels to be interpolated and bad epochs to be rejected. Eye-blinks were removed using independent component analysis from EEGLab⁴². Data were then converted to Current Source Density (CSD).

Rodents

Twelve Long-Evans rats (aged 3-4 months) were trained to perform a delayed response task. Of these, three had microwire arrays in the medial frontal cortex only, three had microwire arrays in both medial frontal cortex and primary motor cortex, and six had cannulae in medial frontal cortex and microwire arrays in motor cortex. Of these six, only three animals had both well-isolated single units and local field potentials that were free of movement artifacts and line noise in the motor cortex. Rats were motivated by regulated access to water, while food was available *ad libitum*. Rats consumed 10-15 ml of water during each behavioral session and additional water (5-10 ml) was provided 1-3 hours after each behavioral session in the home cage. Single housing and a 12 hour light/dark cycle was used; all experiments took place during the light cycle. Rats were maintained at ~90% of their free-access body weights during the course of these experiments, and received one day of free access to water per week. The Animal Care and Use Committee at the John B. Pierce Laboratory approved all procedures. No statistical methods were used to pre-determine sample sizes but our sample sizes are similar to those reported in previous publications^{10,11,43}.

Task

Rats were trained to perform a time-estimation task using standard operant procedures²⁹ and by motivation through regulated access to water. To perform this task correctly, animals had to press and hold a lever for a 1000 ms delay period, and release the lever promptly (within 600 ms) in order to receive a liquid reward (0.15 ml of water). The end of the delay period, or target time, was signaled by a 100 ms 72 dB 8 KHz tone. Response time was defined as the latency between the target time at the end of the delay period and lever release. In

recording sessions, tones were omitted on 50% of trials (catch trials). If animals released the lever prior to the end of the 1000 ms delay or after the 600 ms response window, then these trials were scored as errors (premature or late, respectively), and all behavioral devices (pump, lever and houselight) were extinguished for a 4000-8000 ms inter-trial interval (ITI). No tones occur on premature trials. Our previous work with this task in rats suggests that catch trials do not affect prefrontal delay-related or task-related activity^{10,43} or behavior. As described previously^{10,43} late trials were infrequent (<10% of trials) and excluded from all rodent and human analysis.

Rodent behavioral apparatus

Operant chambers (MedAssociates, St Albans, VT) were equipped with a lever, a drinking tube, and a speaker driven to produce an 8 kHz tone at 72 dB, using audio equipment either from Tucker-Davis Technologies (Alachua, FL) or manufactured in the Instruments Shop at the Pierce Laboratory. Behavioral arenas were housed in sound-attenuating chambers (MedAssociates). On correct responses, water was delivered via a pump (MedAssociates) connected to a standard metal drinking tube (AnCare) via Tygon tubing. Behavioral devices (houselight, pump, click stimulus) were activated after a delay of 100 ms after lever release. Response force was measured using a load cell (part #LCL-454G, Omega Engineering, Stamford, CT, rated to .454 N, or a thin film load cell, part #S100, Strain Measurement Devices, Meriden, CT, rated to 1 N), mounted at the back of the lever.

Medial frontal inactivation

Reversible inactivation of medial frontal cortex was performed according to procedures described previously²⁹. Briefly, 33-gauge cannulae (Plastics One) were implanted bilaterally into the dorsal prelimbic region (coordinates from bregma: AP: +3.2, ml ± 1.4, DV -3.6 @ 10° in the lateral plane) of three fully trained animals via aseptic surgical procedures. One week after surgery, animals were lightly anesthetized with halothane via a nosecone for 7 min and tested in the time-estimation task 45 min after recovery from anesthesia. On the first day of testing, 0.9% saline (Phoenix Scientific, St. Joseph, MO) was infused into medial frontal cortex (control sessions). On the second day of testing, muscimol¹⁰, a GABA-A receptor agonist (Sigma-Aldrich, St Louis, MO), was infused into ACC at 0.1 µg/µl (inactivation sessions). On the third day of testing, animals were run without manipulation. Infusion was conducted by inserting injectors into the guide cannula and 0.5 µl of infusion fluid was delivered per site at a rate of 15 µl/hr (0.25 µl/min) via a syringe infusion pump (KDS Scientific, Holliston, MA). After injection was complete, the injector was left in place for 2 minutes to allow for diffusion. Rats were tested in the simple time-estimation task 45 minutes after the start of the infusions.

Neurophysiological Recordings

Microelectrodes configured in 4×4 arrays of 50 µm stainless steel wires (250 µm between wires; impedance measured in vitro at 100-300 kΩ; Neuroline: New York, NY) were implanted into rat motor cortex (nine animals; of these, six also had cannula in prelimbic cortex; coordinates from bregma: AP: -0.5, ML: ± 2.5-3.5, DV: -1.5 @ -25° in the frontal plane; three had noise in their field potential and were excluded from LFP analyses) according to methods described in detail previously¹⁰. In six animals, microelectrode arrays

were implanted targeting dorsal prelimbic cortex in medial frontal cortex (Three of these also with motor cortex recording electrodes; coordinates from bregma: AP: +3.2, ml \pm 1.4, DV -3.6 @ 10° in the frontal plane; one had noise in its' field potential and was excluded from LFP analyses; Fig 1d). Once experiments were complete, rats were anesthetized and sacrificed by injections of 100 mg/kg sodium pentobarbital and then were transcordially perfused with either 10% formalin or 4% paraformaldehyde. Brains were sectioned on a freezing microtome, mounted on gelatin-subbed slides, and stained for Nissl with thionin.

Neuronal ensemble recordings were made using a multi-electrode recording system (Plexon, Dallas, TX). Putative single neuronal units were identified on-line using an oscilloscope and audio monitor. The Plexon off-line sorter was used to analyze the signals off-line and to remove artifacts. Spike activity was analyzed for all cells that fired at rates above 0.1 Hz. Statistical summaries were based on all recorded neurons. No subpopulations were selected or filtered out of the neuron database. Local field potential was recorded using wide-band boards with bandpass filtered between 0.07 and 8000 Hz. Principal component analysis (PCA) and waveform shape were used for spike sorting. Single units were identified as having 1) consistent waveform shape, 2) separable clusters in PCA space, 3) average amplitude estimated at least three times larger than background activity, 4) a consistent refractory period of at least 2 ms in interspike interval histograms, and 5) consistent firing rates around behavioral events (as measured by a runs test of firing rates across trials around behavioral events; neurons with $|z|$ scores $>$ 4 were considering 'nonstationary' and were excluded). Analysis of neuronal activity and quantitative analysis of basic firing properties were carried out using Stranger (Biographics, Winston-Salem, NC), NeuroExplorer (Nex Technologies, Littleton, MA), and with custom routines for MATLAB. Peri-event rasters and average histograms were constructed around lever release, lever press, and tone offset.

Partial correlation analysis was used to explore the relationship of spiking activity to prior outcome and response time using Spearman's non-parametric rank correlation in MATLAB (function `PARTIALCORR`). This analysis partials out the influence of response time or prior outcome (i.e., if the previous trial was correct or premature) on spike counts using a sliding window starting ± 2 seconds prior to lever press. Statistical significance was assessed by shuffling trial orders 1000 times, and effect size was quantified using the absolute value of Spearman's Rho statistic.

Time-frequency and statistical analysis

For both rats and humans, all post-error analyses were restricted to correct trials immediately after a premature error (occurring before the imperative stimulus was presented). Normality was tested via the Jarque-Bera goodness-of-fit test, and where appropriate, non-parametric displays and statistics were used. Time-frequency calculations were computed using custom-written Matlab routines²¹. Time-frequency measures were computed by multiplying the fast Fourier transformed (FFT) power spectrum of single trial EEG or LFP data with the FFT power spectrum of a set of complex Morlet wavelets

(defined as a Gaussian-windowed complex sine wave: $e^{i2\pi t f} e^{-\frac{t^2}{2\pi\sigma^2}}$, where t is time, f is frequency (which increased from 1 to 50Hz in 50 logarithmically spaced steps), and defines the width (or "cycles") of each frequency band, set according to $4/(2\pi f)$), and taking the

inverse FFT. The end result of this process is identical to time-domain signal convolution, and it resulted in: 1) estimates of instantaneous power (the magnitude of the analytic signal), defined as $Z[t]$ (power time series: $p(t) = \text{real}[z(t)]^2 + \text{imag}[z(t)]^2$); and, 2) phase (the phase angle) defined as $= \arctan(\text{imag}[z(t)]/\text{real}[z(t)])$. Each epoch was then cut in length surrounding the event of interest (-500 to $+500$ ms). Power was normalized by conversion to a decibel (dB) scale ($10 \cdot \log_{10}[\text{power}(t)/\text{power}(\text{baseline})]$), allowing a direct comparison of effects across frequency bands. The baseline for each frequency consisted of the average power from -500 to -300 ms prior to the onset of each trial.

Inter-site phase coherence was used to measure the consistency of phase values for a given frequency band across two different recording sites. Inter-site phase coherence values vary from 0 to 1, where 0 indicates random phases at that time-frequency point between channels, and 1 indicates identical phase values at that time-frequency point between channels. Spike triggered averages were calculated by plotting average field potential around post-error and post-correct spikes for each neuron and field. To look at the time-frequency component of interactions between individual spikes and the field potential, we applied spike-field coherence analysis using the Neurospec toolbox²⁸, in which multivariate Fourier analysis was used to extract phase-locking among spike trains and local field potentials. As above, phase-locking coherence values varied from 0 to 1, where 0 indicates no coherence, and 1 indicates perfect coherence. Fractional coherence was plotted by scaling coherence by power spectra. Statistical significance between conditions was determined by computing pixel-wise paired sample t-tests between post-error and post-correct trials. For phase consistency, conditions were matched for epoch counts by response latency matching post-error trials with post-correct trials.

For response latency analysis in medial frontal inactivation sessions (Fig 5), comparisons were restricted to sequences of trials preceded by correct or premature responses. Response latencies could be negative because premature responses were included. Comparisons included 59 ± 10 correct / 13 ± 1 error trials in control and on 18 ± 12 correct / 16 ± 2 error trials in inactivation sessions.

Correlations between trial-by-trial EEG/LFP and response latency were computed within each condition for each participant separately using non-parametric Spearman's rho values. Differences in trial-to-trial EEG/LFP-RT patterns were investigated with paired samples t-tests of the sample rho. We displayed the full time-frequency plots of human data for comparison with findings from the rat, yet we had extremely strong Regions of Interest (ROIs) for expected findings based on the underlying frequency in the human ERP, the temporal-frequency effects in the rat, and similar findings explicitly detailed in our previous work²¹. On post-error trials, enhanced medial frontal activities were proposed to occur after the tone specifically in the theta (4-8 Hz) band, and response-locked correlations with response times in a slightly lower and broader range⁴¹. Significant differences for spike-field coherence were computed from 95% confidence intervals and verified by bootstrapping time-shuffled data.

Supplementary Material

Refer to Web version on PubMed Central for supplementary material.

Acknowledgements

The authors would like to thank Sean Masters for help with human data acquisition, to Nicole Horst for technical editing, and to Guangyu Robert Yang for help with spike-field coherence code and simulations. This work was funded by an NINDS K08 to NSN, NIH grant MH080066-01 and NSF grant 1125788 to MJF, and NIH P01-AG030004-01A1 and NSF 1121147 to ML.

References

1. Bellman R, Kalaba R. A MATHEMATICAL THEORY OF ADAPTIVE CONTROL PROCESSES. *Proc. Natl. Acad. Sci. U.S.A.* 1959; 45:1288–1290. [PubMed: 16590506]
2. Ridderinkhof KR, Ullsperger M, Crone EA, Nieuwenhuis S. The Role of the Medial Frontal Cortex in Cognitive Control. *Science*. 2004; 306:443–447. [PubMed: 15486290]
3. Holroyd CB, Coles MGH. The neural basis of human error processing: reinforcement learning, dopamine, and the error-related negativity. *Psychol Rev.* 2002; 109:679–709. [PubMed: 12374324]
4. Rushworth MFS, Behrens TEJ. Choice, uncertainty and value in prefrontal and cingulate cortex. *Nature Neuroscience*. 2008; 11:389–397. [PubMed: 18368045]
5. vanMeel CS, Heslenfeld DJ, Oosterlaan J, Sergeant JA. Adaptive control deficits in attention-deficit/hyperactivity disorder (ADHD): the role of error processing. *Psychiatry Res.* 2007; 151:211–220. [PubMed: 17328962]
6. Velligan DI, Ritch JL, Sui D, DiCocco M, Huntzinger CD. Frontal Systems Behavior Scale in schizophrenia: relationships with psychiatric symptomatology, cognition and adaptive function. *Psychiatry Res.* 2002; 113:227–236. [PubMed: 12559479]
7. Fitzgerald KD, et al. Error-related hyperactivity of the anterior cingulate cortex in obsessive-compulsive disorder. *Biol. Psychiatry*. 2005; 57:287–294. [PubMed: 15691530]
8. Miller EK, Cohen JD. An integrative theory of prefrontal cortex function. *Annu. Rev. Neurosci.* 2001; 24:167–202. [PubMed: 11283309]
9. Robbins T. Shifting and stopping: fronto-striatal substrates, neurochemical modulation and clinical implications. *Philosophical Transactions of the Royal Society B: Biological Sciences*. 2007; 362:917–932.
10. Narayanan NS, Laubach M. Top-down control of motor cortex ensembles by dorsomedial prefrontal cortex. *Neuron*. 2006; 52:921–931. [PubMed: 17145511]
11. Narayanan NS, Laubach M. Neuronal correlates of post-error slowing in the rat dorsomedial prefrontal cortex. *J. Neurophysiol.* 2008; 100:520–525. [PubMed: 18480374]
12. Carter CS, et al. Anterior Cingulate Cortex, Error Detection, and the Online Monitoring of Performance. *Science*. 1998; 280:747–749. [PubMed: 9563953]
13. Sheth SA, et al. Human dorsal anterior cingulate cortex neurons mediate ongoing behavioural adaptation. *Nature*. 2012; 488:218–221. [PubMed: 22722841]
14. Rabbitt PM. Errors and error correction in choice-response tasks. *J Exp Psychol.* 1966; 71:264–272. [PubMed: 5948188]
15. Danielmeier C, Ullsperger M. Post-error adjustments. *Front Psychol.* 2011; 2:233. [PubMed: 21954390]
16. Dutilh G, et al. Testing theories of post-error slowing. *Atten Percept Psychophys.* 2012; 74:454–465. [PubMed: 22105857]
17. Modirrousta M, Fellows LK. Dorsal medial prefrontal cortex plays a necessary role in rapid error prediction in humans. *J. Neurosci.* 2008; 28:14000–14005. [PubMed: 19091989]
18. Hampson RE, et al. Facilitation and restoration of cognitive function in primate prefrontal cortex by a neuroprosthesis that utilizes minicolumn-specific neural firing. *J Neural Eng.* 2012; 9:056012. [PubMed: 22976769]

19. McClintock SM, Freitas C, Oberman L, Lisanby SH, Pascual-Leone A. Transcranial magnetic stimulation: a neuroscientific probe of cortical function in schizophrenia. *Biol. Psychiatry*. 2011; 70:19–27. [PubMed: 21571254]
20. Kornblum S. Simple reaction time as a race between signal detection and time estimation: A paradigm and a model. *Perception and Psychophysics*. 1973; 13:108–112.
21. Cavanagh JF, Cohen MX, Allen JJB. Prelude to and resolution of an error: EEG phase synchrony reveals cognitive control dynamics during action monitoring. *J. Neurosci*. 2009; 29:98–105. [PubMed: 19129388]
22. Buzsáki, G. *Rhythms of the Brain*. Oxford University Press; 2011. at <http://www.oup.com/us/catalog/general/subject/Medicine/Neuroscience/?view=usa&ci=9780199828234>
23. Fujisawa S, Amarasingham A, Harrison MT, Buzsáki G. Behavior-dependent short-term assembly dynamics in the medial prefrontal cortex. *Nature Neuroscience*. 2008; 11:823–833. [PubMed: 18516033]
24. Narayanan NS, Kimchi EY, Laubach M. Redundancy and synergy of neuronal ensembles in motor cortex. *J. Neurosci*. 2005; 25:4207–4216. [PubMed: 15858046]
25. Laubach M, Wessberg J, Nicolelis MA. Cortical ensemble activity increasingly predicts behaviour outcomes during learning of a motor task. *Nature*. 2000; 405:567–571. [PubMed: 10850715]
26. Stefanics G, et al. Phase entrainment of human delta oscillations can mediate the effects of expectation on reaction speed. *J. Neurosci*. 2010; 30:13578–13585. [PubMed: 20943899]
27. Womelsdorf T, Johnston K, Vinck M, Everling S. Theta-activity in anterior cingulate cortex predicts task rules and their adjustments following errors. *Proc. Natl. Acad. Sci. U.S.A.* 2010; 107:5248–5253. [PubMed: 20194767]
28. Rosenberg JR, Amjad AM, Breeze P, Brillinger DR, Halliday DM. The Fourier approach to the identification of functional coupling between neuronal spike trains. *Prog. Biophys. Mol. Biol.* 1989; 53:1–31. [PubMed: 2682781]
29. Narayanan NS, Horst NK, Laubach M. Reversible inactivations of rat medial prefrontal cortex impair the ability to wait for a stimulus. *Neuroscience*. 2006; 139:865–876. [PubMed: 16500029]
30. Allen TA, et al. Imaging the spread of reversible brain inactivations using fluorescent muscimol. *J. Neurosci. Methods*. 2008; 171:30–38. [PubMed: 18377997]
31. vonStein A, Chiang C, König P. Top-down processing mediated by interareal synchronization. *Proc. Natl. Acad. Sci. U.S.A.* 2000; 97:14748–14753. [PubMed: 11121074]
32. Cavanagh JF, Zambrano-Vazquez L, Allen JJB. Theta lingua franca: a common mid-frontal substrate for action monitoring processes. *Psychophysiology*. 2012; 49:220–238. [PubMed: 22091878]
33. Cavanagh JF, et al. Subthalamic nucleus stimulation reverses mediofrontal influence over decision threshold. *Nat. Neurosci*. 2011; 14:1462–1467. [PubMed: 21946325]
34. Allman JM, Hakeem A, Erwin JM, Nimchinsky E, Hof P. The anterior cingulate cortex. The evolution of an interface between emotion and cognition. *Ann. N. Y. Acad. Sci.* 2001; 935:107–117. [PubMed: 11411161]
35. Davidson RJ, Pizzagalli D, Nitschke JB, Putnam K. Depression: perspectives from affective neuroscience. *Annu Rev Psychol*. 2002; 53:545–574. [PubMed: 11752496]
36. Wise SP. Forward frontal fields: phylogeny and fundamental function. *Trends Neurosci*. 2008; 31:599–608. [PubMed: 18835649]
37. Vertes RP, Hoover WB, Do Valle AC, Sherman A, Rodriguez JJ. Efferent projections of reuniens and rhomboid nuclei of the thalamus in the rat. *J. Comp. Neurol*. 2006; 499:768–796. [PubMed: 17048232]
38. Dzirasa K, et al. Noradrenergic control of cortico-striato-thalamic and mesolimbic cross-structural synchrony. *J. Neurosci*. 2010; 30:6387–6397. [PubMed: 20445065]
39. Newman EL, Gupta K, Climer JR, Monaghan CK, Hasselmo ME. Cholinergic modulation of cognitive processing: insights drawn from computational models. *Front Behav Neurosci*. 2012; 6:24. [PubMed: 22707936]
40. Lee TG, D'Esposito M. The dynamic nature of top-down signals originating from prefrontal cortex: a combined fMRI-TMS study. *J. Neurosci*. 2012; 32:15458–15466. [PubMed: 23115183]

41. Cohen MX, Cavanagh JF. Single-trial regression elucidates the role of prefrontal theta oscillations in response conflict. *Front Psychol.* 2011; 2:30. [PubMed: 21713190]
42. Delorme A, Makeig S. EEGLAB: an open source toolbox for analysis of single-trial EEG dynamics including independent component analysis. *J. Neurosci. Methods.* 2004; 134:9–21. [PubMed: 15102499]
43. Narayanan NS, Laubach M. Delay activity in rodent frontal cortex during a simple reaction time task. *J. Neurophysiol.* 2009; 101:2859–2871. [PubMed: 19339463]

Author Manuscript

Author Manuscript

Author Manuscript

Author Manuscript

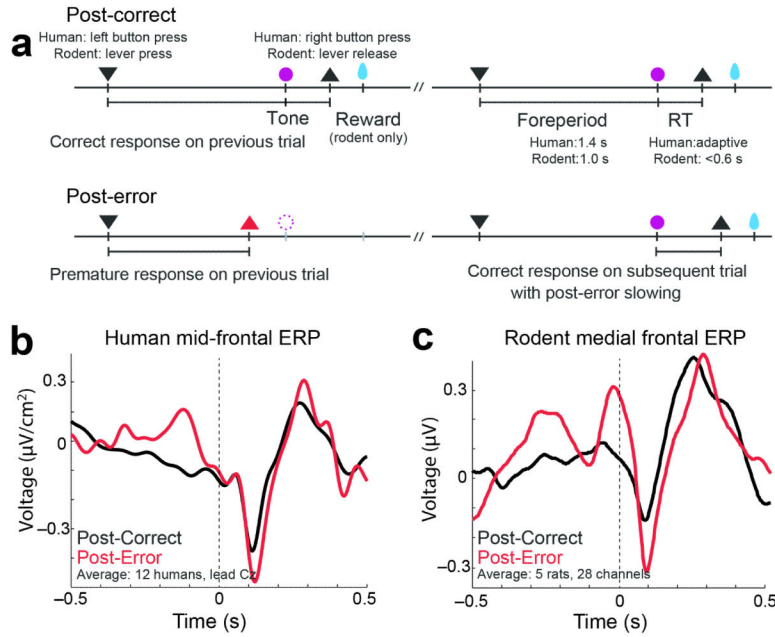


Figure 1. Common mechanisms of medial frontal cortical oscillations during adaptive control in rats and humans. a) Sequences of events in the time-estimation task on post-correct vs post-error trials (black). All analyses here are restricted to correct trials as a function of prior outcome. ▼ - press; ● - tone; ▲ - release, and ● - reward. Imperative tones occurred at the target time on 50% of trials. b) Average event-related potentials over mid-frontal cortex (electrode Cz) in humans aligned to the target time. Amplitudes were significantly increased on post-error (red) vs. post-correct (black) trials. c) Rodent medial frontal field potentials were also significantly increased on post-error (red) vs. post-correct (black) trials, and highly similar to humans. Data is from 28 medial frontal channels in 5 rats and is aligned to the target time.

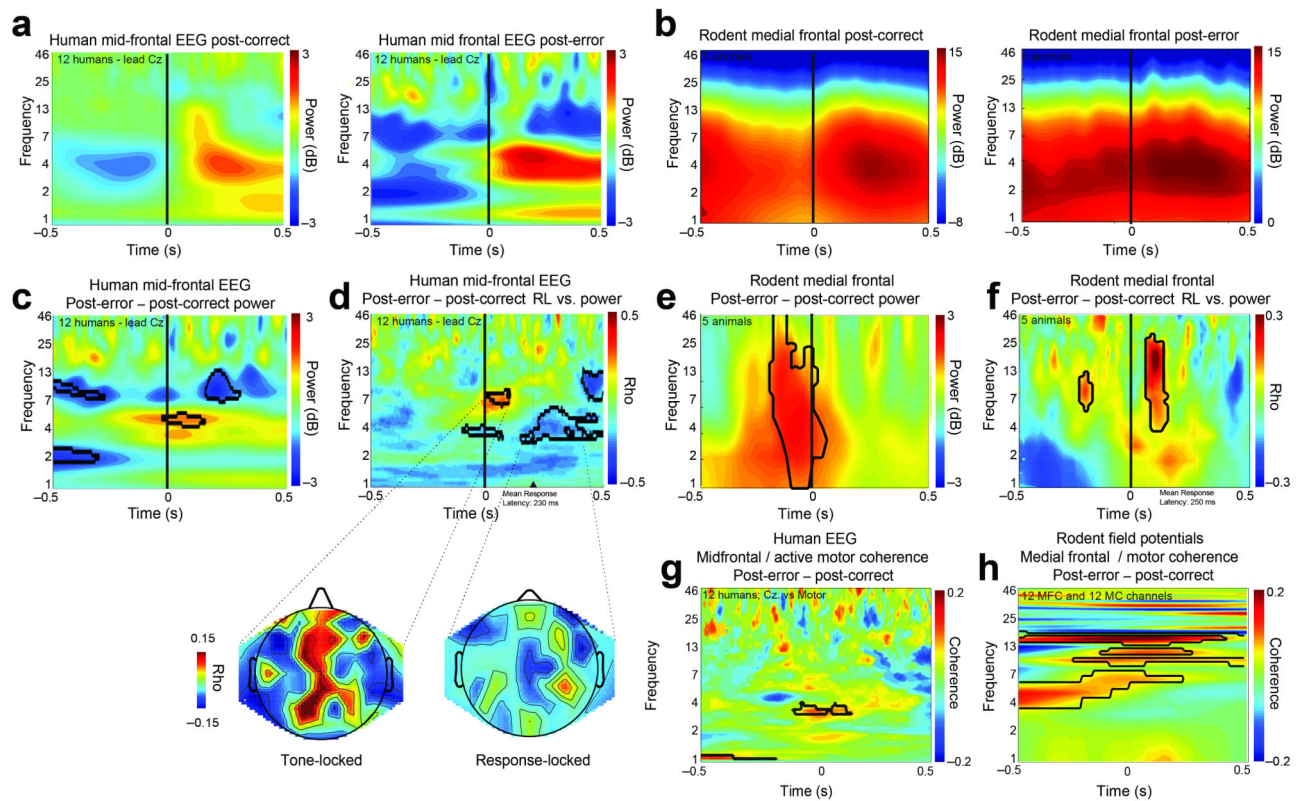


Figure 2.

Time-frequency analysis reveals enhanced low-frequency power after errors. a) Humans: on post-correct trials, there was less low-frequency power than on post-error trials. b) Rodents: on post-correct trials, there was less low-frequency power than on post-error trials. c) Humans: direct comparison of post-error and post-correct trials revealed stronger theta modulation to the imperative tone on post-error trials. d) Humans: trial-to-trial variation in low frequency EEG signals was significantly correlated with subsequent response latency (electrode Cz). Current source density of scalp topographies (shown below) revealed that these effects were prominent over medial frontal regions. b) Rodents: similar patterns were seen in rodents, although broader bands of low-frequency modulation were observed. e) Rodents: direct comparison of post-error and post-correct trials revealed dramatically stronger low-frequency modulation to the imperative tone on post-error trials. f) Rodents: trial-to-trial variation in 4-25 Hz frequencies were strongly correlated with subsequent response latency. Time aligned to the target time; black contours indicate significant differences via a t-test between post-error and post-error trials ($p < 0.05$) or Spearman's (non-parametric) correlations ($p < 0.05$). g) Humans: midfrontal and motor sites had significantly more low-frequency coherence on post-error compared to post-correct trials. h) Rodents: A similar pattern was observed in rodents between 12 medial frontal and 12 motor cortex channels in three rats. Time for g-h aligned to trial initiation; black contours indicate significant differences via a t-test between post-error and post-error trials ($p < 0.05$).

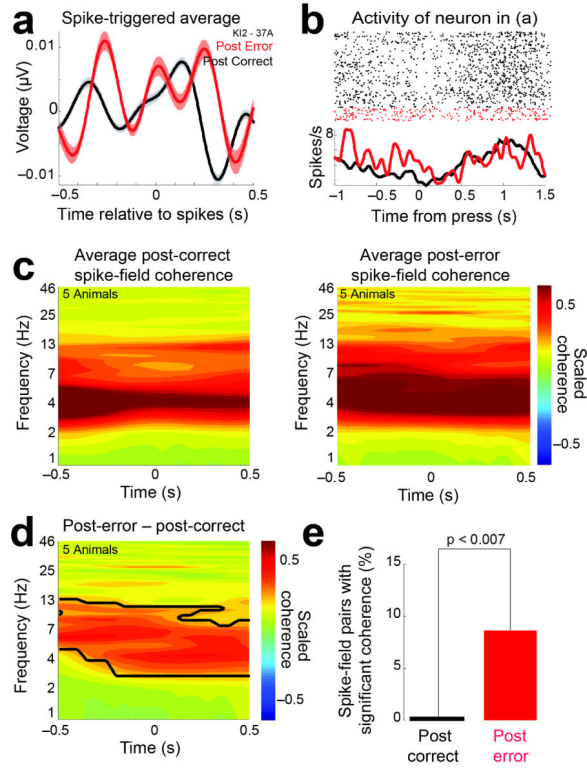


Figure 3. Medial frontal single neuron spiking is coupled with low-frequency oscillations. a) Spike-triggered average of a medial frontal neuron where local field potentials are averaged across all spikes within 2 seconds of lever press for a single neuron. For this neuron, the spike-triggered average revealed robust low-frequency oscillations on post-error trials compared to post-correct trials. b) Peri-event raster of the neuron in a) revealed different patterns of activity after errors as well as low-frequency oscillations in firing rates. c) Spike-field coherence to post-correct and post-error trials. d) Post-error trials were characterized by enhanced low-frequency spike-field coupling. e) 9% of medial frontal neurons had significant low-frequency (below 12 Hz) spike-field coherence on post-error trials, compared to no significant spike-field pairs on post-correct trials. Time aligned to the target time (\blacktriangle - release); black contours indicate significant differences via a t-test between post-error and post-error trials ($p < 0.05$).

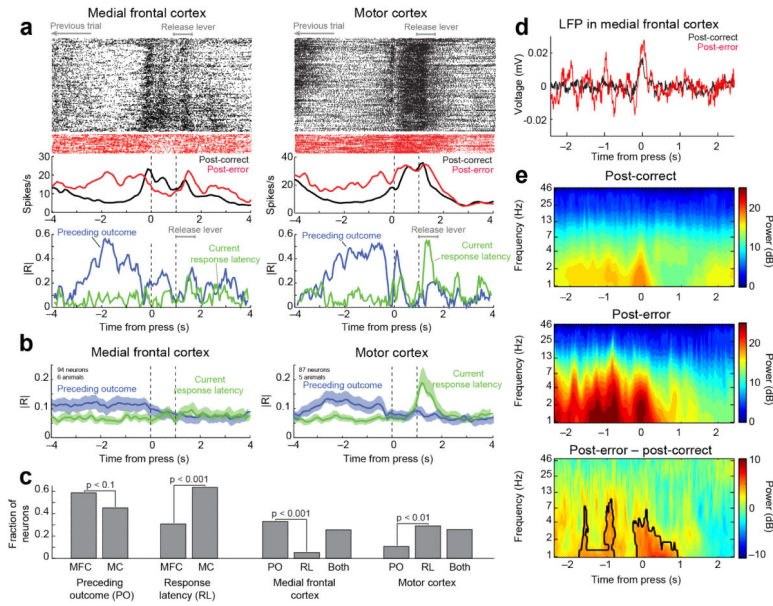


Figure 4. Encoding of previous outcomes in the medial frontal and motor cortices. a) Examples of spike activity and correlation coefficients from the partial correlation analysis are shown for neurons in the medial frontal and motor cortices. b) Group summary for the sliding-window partial correlation analysis revealed that neurons in both cortical areas were sensitive to the previous outcome (in blue) and that only neurons in the motor cortex were sensitive to variations in response latency (in green). Error bars represent SEM. c) Fractions of neurons that were selective to the previous outcome and current response latency and that were sensitive to either or both of these behavioral factors are summarized in the lower plot. Significance was assessed over all data windows (± 2 sec around the press event). d) Spiking correlates of previous outcomes were accompanied by increased low-frequency oscillations in the field potential, as was apparent in the trial-averaged ERP and event-related spectral power. e) Medial frontal cortex local field potentials had prominent low-frequency modulation around the time of the response; plots aligned to trial initiation; black contours indicate significant differences via a t-test between post-error and post-error trials ($p < 0.05$)

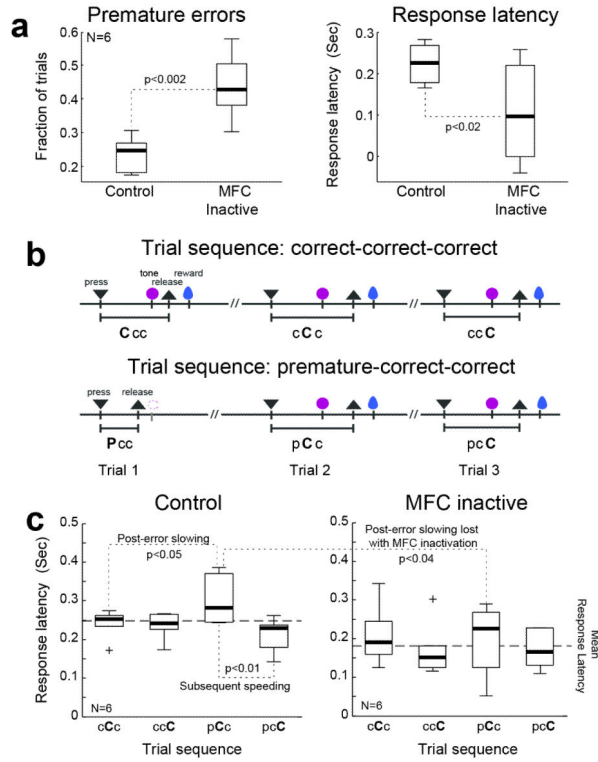


Figure 5. Loss of adaptive control following inactivation of the medial frontal cortex. a) Reversible inactivation of the medial frontal cortex in 6 rats increased the fraction of trials with premature responses and reduced the overall response time. b) Given erratic performance in the inactivation sessions with runs of premature errors, it was essential to confirm that effects on response latency adjustments would be found in controlled sequences of trials in which rats made two consecutive correct responses after making either a correct response or premature error response. c) Analysis of the trial sequences revealed clear evidence for slowing of response latencies after premature errors and a subsequent speeding in the control session (saline infused into the medial frontal cortex). This was not observed in sessions with medial frontal cortex inactivated. Inactivation of medial frontal cortex also led to an overall speeding of responses and eliminated the post-error slowing and subsequent speeding after the corrected response. Boxes – IQR; Whiskers 1.5x IQR

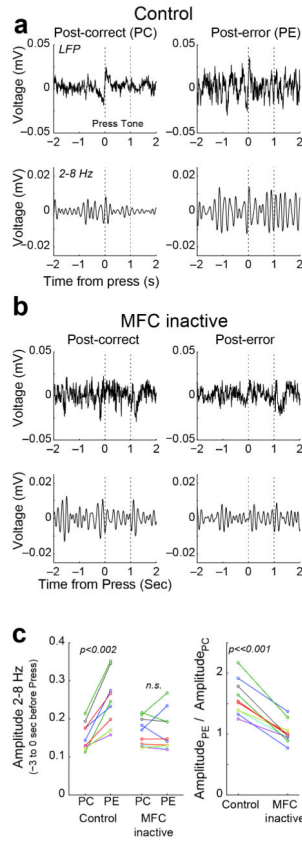
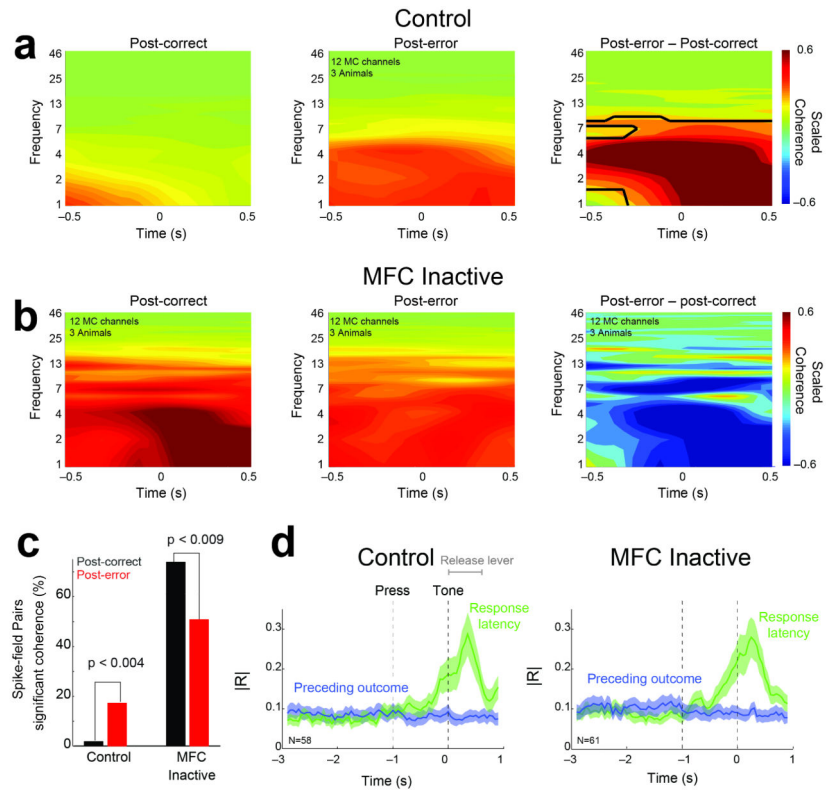


Figure 6. Inactivation of medial frontal cortex eliminated post-error increases in low-frequency oscillations in motor cortex. a) Peri-event averages of wideband field potentials (top row) and bandpass filtered signals (2-8 Hz; lower row) are shown from the motor cortex of one rat. In the control session, low frequency oscillations were elevated on post-error trials. b) Sessions with medial frontal cortex inactivated. C) Z-transformed amplitude in the range between 2 and 8 Hz was measured using the Hilbert transform. Medial inactivation caused low frequency oscillations to become equivalent on the post-correct and post-error trials. This effect was found every field potential examined from three rats.

**Figure 7.**

Rat medial frontal cortex directly influences post-error low-frequency oscillations in motor cortex in the service of adaptive control. a) In control sessions, low-frequency spike-field coherence in motor cortex on post-correct trials was less prominent than on post-error trials, as was apparent in comparisons of spike-field coherence between post-error and post-correct trials (right column). b) Medial frontal inactivation increase post-correct spike-field coherence and abolished differences between post-error and post-correct trials (right column). Black contours indicate significant differences via a t-test between post-error and post-correct trials ($p < 0.05$); see Fig S5 for comparison between control and medial frontal inactivation sessions. c) Medial frontal inactivation increased the numbers of neurons with post-significant spike-field coherence on post-correct trials. These data suggest that with medial frontal inactivation, low-frequency coherence is no longer specific to post-error trials. Error bars represent SEM. d) Changes to spike-field coupling occurred in the absence of any effects of medial frontal inactivation on the sensitivity of the motor cortical neurons to the prior behavioral outcome or response latency; note that this is a subset of data in Fig 4 with slightly less predictive power for previous outcome.